Journal of Applied Polymer Science

The Influence of Mechanical Cold Drawing and Drawing Velocity on the Molecular Structure of Isotactic Polypropylene Fiber

T. Z. N. Sokkar, M. A. El-Bakary, A. M. Ali
Physics Department, Faculty of Science, Mansoura University, Mansoura 35516, Egypt
Correspondence to: M. A. El-Bakary (E-mail: elbakary2@yahoo.com)

ABSTRACT: The main goal of this work study is to study the influence of mechanical cold drawing and drawing velocity on the molecular orientation and physical structure parameters of isotactic polypropylene, iPP, fibers. A Video Opto- Mechanical device (VOM) attached with automatic multiple-beam interferometric technique was used to cold draw iPP fibers at different draw ratio and drawing velocity. The molecular structure of iPP fiber was characterized by measuring the refractive indices, birefringence, optical orientation function, orientation angle, the percentage of the volume fraction of amorphous and crystalline regions, density and the mean square density fluctuation. The obtained microinterferograms of multiple beam interference fringes were enhanced and the noises were removed by using Fourier transform method. The obtained contour lines were analyzed via a software program for fiber refractive index determination. The results show that the drawing velocity has a less effect than the draw ratio on the molecular structure of iPP fiber. The contour lines of microinterferograms are given for illustration. © 2012 Wiley Periodicals, Inc. J. Appl. Polym. Sci. 000: 000–000, 2012

KEYWORDS: drawing velocity; birefringence; optical orientation; crystallinity; VOM device; iPP fiber

Received 14 October 2011; accepted 21 February 2012; published online
DOI: 10.1002/app.37559

INTRODUCTION

Isotactic polymers are composed of isotactic macromolecules. In isotactic macromolecules all the substituents are located on the same side of the macromolecular backbone. Isotactic polymers are usually semicrystalline and often form a helix configuration. Polypropylene formed by Ziegler-Natta catalysis is an isotactic polymer.[1] Isotactic polypropylene, iPP, is a polymorphic polymer having a tendency to crystallize in numerous crystal modification, such as monoclinic, hexagonal and triclinic. Because of its nonpolar, inert nature, the use of homo-iPP in composite material is limited.[2] Tacticity in isotactic polypropylene refers to the relative orientation of each methyl group to the neighboring methyl groups affecting local chain symmetry which affects crystallization and packing. Each methyl group takes up space and constrains backbone bending. Isotactic refers to methyl groups on one side only.[3] Isotactic polyproplene iPP has entertained global commercial utilization since its inception because of the balance in its properties and cost-effectiveness.[4]

The drawing process is of considerable importance in polymer engineering. The objective of this process is to produce a final fiber of uniform cross-section in which the tensile strength is higher than the original unoriented polymer fiber.[5] The influence of the draw ratio upon the optical and structure changes occurring in the synthetic fibers is also indicated. Molecules are oriented parallel to the fiber axis, and the drawing may produce a fringed fibril structure with the molecules lying parallel to the axis of the crystalline fiber. The initial effect of the fibrils is thus by increasing the transverse orientation of the molecules. If the drawing process is continued, this will be followed by a change to longitudinal orientation of the molecules.[6] Another important factor in the cold drawing process is the drawing velocity. According to the viscoelastic mechanism, an increase in the drawing velocity should bring about an increase in drawing tension and stress. The influence of drawing velocity is less simple. An increase of the drawing velocity is accompanied by lower effective orientations.[7]

The most important structural consequence of drawing is the axial orientation of macromolecules and crystallites. The structural effect of drawing is associated with phase transitions: crystallization, destruction of crystals, crystal transformation. Crystallinity, depending on the drawing conditions, can either increase or decrease in the course of drawing. Physical characteristics related primarily to crystallinity, such as density, behave similarly. Consequently, orientation leads to the anisotropy of

various physical characteristics and optical properties such as birefringence.[7]

Interferometric techniques have been an accurate and available techniques for measuring the refractive indices and birefringence of polymer synthetic fibers.[8] They were extensively used for investigating and detecting the influence of mechanical drawing on the optical, orientation and structural properties of fibers.[9,10] A Video Opto-Mechanical device (VOM)[11] was designed in order to dynamically determine the mechanical, optical, and structural properties of fibers at different uniform drawing velocities. The threshold cold drawing velocity was detected to avoid necking deformation. The VOM device attached to a multiple-beam interferometric system is an accurate and efficient technique in the field of interferometery applied for fibers monitoring.

The main goal of this work is to study the influence of mechanical cold drawing and drawing velocity on the molecular orientation and physical structure parameters of isotactic polypropylene, iPP, fibers. A VOM device attached with automatic multiple-beam interferometric technique were used to stretch iPP fibers at different draw ratio and drawing velocity. The molecular structure of iPP fiber was characterized by measuring the refractive indices, birefringence, optical orientation function, orientation angle, the percentage of the volume fraction of amorphous and crystalline regions, density and the mean square density fluctuation.

MATERIALS

The isotactic polypropylene fibers, iPP, were prepared as spun using a Fiber Extrusion Technology (FET) melt spinning machine at the center for Technical Textiles, University of Leeds, UK.[1] The pump speed was set to 15 rpm at spinning temperature 245°C. The number of spinneret holes was 20 with a diameter of 0.8 mm and 3.2 mm in length. The take-up velocity varied from 200 to 1000 m/min. The average initial diameter of the fibers are 100 μm. The linear density of the used sample was 32.6 tex and the tenancy was 101.11 mN/tex.[12]

THEORETICAL CONSIDERATIONS

Multiple-beam Fizeau fringes in transmission is an accurate technique for measuring the refractive and birefringence of fibers.[8] When light vibrating parallel to the fiber axis, the refractive index, $n^{\|}$, is given by:

$$n^{\|} = n_L + \frac{F^{\|}\lambda}{2bA} \tag{1}$$

where n_L is the refractive index of the immersion oil, $F^{\|}$ is the area under the fringe shift, λ is the wavelength of the incident light, A is the cross sectional area of the fiber, and b is the interfering spacing. An analogue formula, for determining $n^{\perp}$, can be used when light vibrating perpendicular to the fiber axis. The birefringence, Δn, is given by:

$$\Delta n = n^{\|} - n^{\perp} \tag{2}$$

For a drawn fiber where the molecules are considered to be aligned with the draw direction but only randomly arranged in the transverse section, the optical properties of the system can be specified by only two refractive indices, $n^{\|}$ parallel to the fiber and $n^{\perp}$ perpendicular to the fiber axis. The overall orientation factor $F(\theta)$ is related to the refractive index difference by the relation[13]:

$$F(\theta) = \frac{n^{\|} - n^{\perp}}{\Delta_o} \tag{3}$$

where Δ_o is the intrinsic maximum birefringence which corresponds to the case where all the molecules are perfectly aligned. The value of Δ_o for isotactic polypropylene fiber was taken to be 0.045.[14] The optical orientation angle θ can be found using Hermans orientation factor form the following equation[14]:

$$\theta = \sin^{-1}\left(\frac{2}{3}(1 - F(\theta))\right)^{\frac{1}{2}} \tag{4}$$

where θ being the angle between the polymer chain and the fiber axis. If all polymer chains were aligned parallel to the fiber axis.

The density values were used to estimate of the volume fraction of crystalline regions χ_v for isotactic polypropylene, iPP, fibers using the following equation[14]:

$$\chi_v = \frac{(\rho - \rho_a)}{(\rho_c - \rho_a)} \tag{5}$$

where ρ_c and ρ_a are the densities of the crystalline and amorphous regions, ρ_c = 0.936 g/cm^3 and ρ_a =0.858 g/cm^3 for isotactic polypropylene, iPP, fibers.[15,16] The density ρ of iPP fibers is calculated from the following relation[17];

$$\rho = \frac{\bar{n} - 0.9374}{0.6273} \tag{6}$$

where $\bar{n}$ is the average refractive index. Using the following equation, the average refractive index can be calculated:

$$\bar{n} = \frac{1}{2}(n^{\|} + n^{\perp}) \tag{7}$$

The volume fraction of the amorphous regions, $1-\chi_v$ for isotactic polypropylene, iPP, fibers can be calculated using the following equation:

$$1 - \chi_v = 1 - \frac{(\rho - \rho_a)}{(\rho_c - \rho_a)} \tag{8}$$

For two phase structure consisting of amorphous and crystalline regions with densities ρ_a and ρ_c, respectively. The mean square density fluctuation $\langle\eta^2\rangle$ can be calculated from the following equation[18]

$$\langle\eta^2\rangle = (\rho_c - \rho_a)^2\chi_v(1 - \chi_v) \tag{9}$$

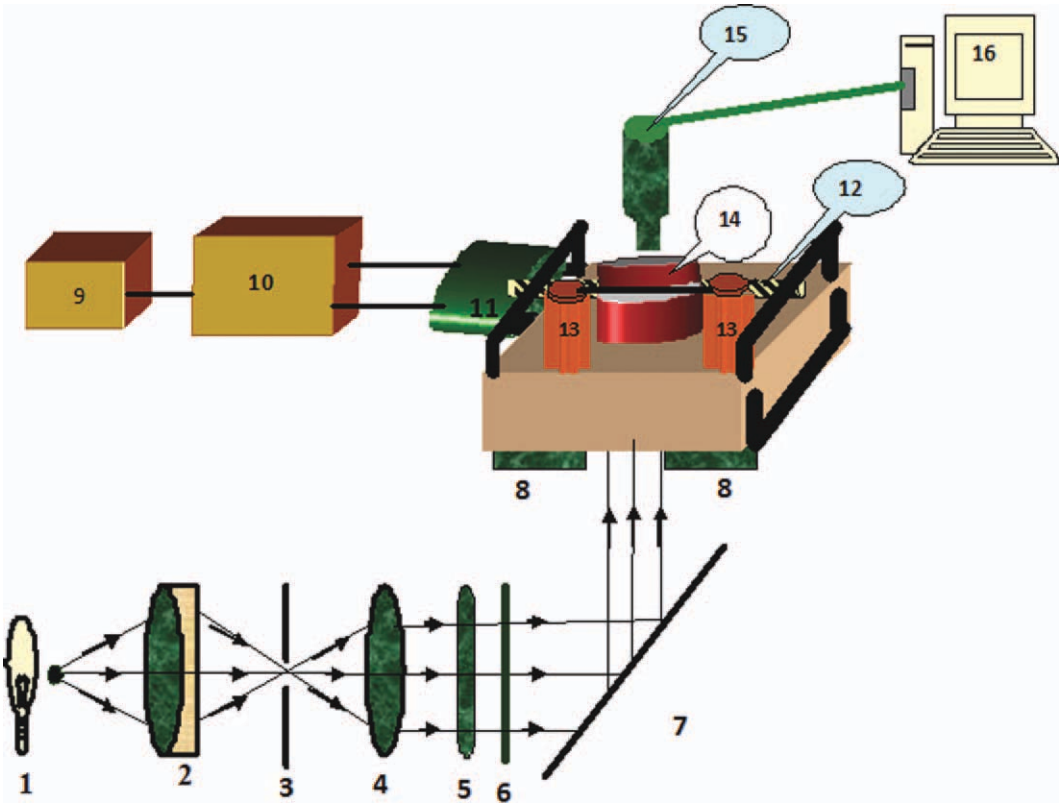

Figure 1. A schematic diagram of the setup of video opto-mechanical device(11) Stepper motor, (12) Bidirectional driving axis, (13) Two gear boxes, (VOM), in which; (1) Spectrum lamp, (2) Condenser lens, (3) Iris dia-(14) Silvered liquid wedge interferometer, (15) CCD micro- camera, (16) phragm, (4) Collimating lens, (5) Polarizer, (6) Monochromatic filter,computer unit. [Color figure can be viewed in the online issue, which is Reflector, (7) Microscope stage, (8) DC battery, (9) Stepper motor interface,available at wileyonlinelibrary.com.]

EXPERIMENTAL TECHNIQUE

A VOM device is a precise and an efficient technique in the field of interferometery for monitoring the mechanical properties of fibers.[11] The (VOM) setup used in this work as shown in Figure 1 consists of three units, Interferometric unit; this unit is an optical system for producing multiple-beam Fizeau fringes in transmission. The arrangement of the unit is described elsewhere.[8] Mechanical unit, this unit is used for drawing the fiber under study and controlling the velocity of drawing. The components and arrangement of this unit was described before.[11] The equation for determining the draw ratio in terms of the stepper motor velocity is given by[11]:

$$\mathrm{DR} = \frac{2\,M}{L} f\,t + 1 \tag{10}$$

where DR is the draw ratio, M is the machine constant (drawing resolution of the machine), f is the frequency of rotation in steps/s, t is time of the frame selected, and L is the initial (undrawn) length of the fiber sample. The drawing velocity using this unit is given by[11]:

$$V = 2\,Mf \quad \mathrm{cm/s} \tag{11}$$

Computerized unit: This unit consists of a Sony CCD micro-camera, digital monitor, and PC computer with software programs controlling the draw ratio, the drawing velocity, and online recording and analyzing the multiple-beam interference microinterferograms. This unit makes the experimental technique be online system for measurement.

The designed (VOM) device was previously calibrated in order to determine the draw ratio of the fiber directly from the recorded video film. Sokkar et al.[11] showed the calibration curve of the device (the variation of the draw ratio with the time of drawing at different drawing velocity).

The video opto-mechanical device (VOM) attached with the automated system for producing multiple-beam Fizeau fringes in transmission was used to determine the optical properties during the online drawing of a sample of isotactic polypropylene, iPP, fibers.

A sample of iPP fiber with a certain length is fixed from its ends with the two gear boxes and mounted on the lower optical flat of the wedge interferometer. The fiber is immersed in a suitable liquid with refractive index $n_L = 1.5001$, close to the parallel refractive index of the fiber, at temperature ($T = 30^{\circ}\mathrm{C}$). The mechanical system is transferred to the optical microscope. A parallel beam of polarized monochromatic light is incident perpendicular to the liquid wedge interferometer, which is

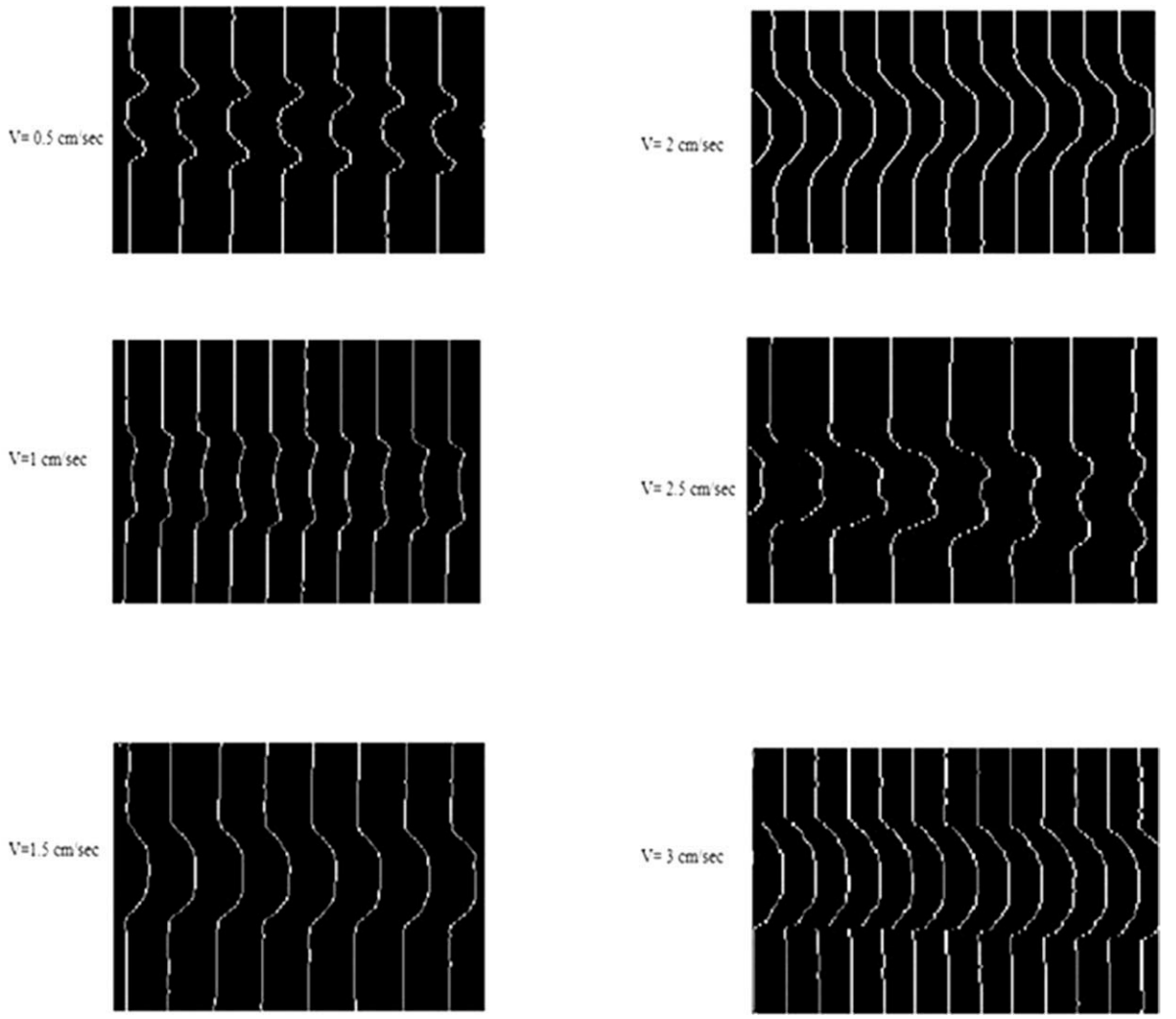

Figure 2. Examples of the contour lines obtained dynamically of the some microinterferograms of iPP fibers at different drawing velocity when light vibrating parallel to the fiber axis at draw ratio equals 5.5.

adjusted in such a way that the fiber axis is exactly perpendicular to the interference fringes in the liquid region. The wavelength of monochromatic light used is 546.1 nm. The stepper motor velocity was adjusted using the software program installed in the computer system. The drawing velocity was adjusted to be 0.5 cm/s. The CCD camera was adjusted to capture the video output images from the microscope field without stopping. Also, the CCD camera was adjusted to capture 25 frames/s during the drawing process of iPP fibers. The obtained video film is cut into separate images to deal with each frame individual. The draw ratio for each frame was calculated using the VOM calibration curve.[11]. The draw ratios values was selected between 2 and 6 with step 0.5 for these investigations. This film is digitized directly via the digitizer frame grabber. The images of the cut frames were enhanced and the noise was removed by using Fourier transform method. The obtained contour lines were analyzed via a software program for fiber refractive index determination.[18] Another samples of iPP fiber was fixed in the VOM device and transferred to the microscope stage. The same immersion oil and wavelength of the incident light beam was used. The drawing velocity was adjusted for each sample to be vary from 1 cm/s to 3.5 cm/s with step 0.5 cm/s. By the same manner before the obtained video film at each drawing velocity value was cut into frames the draw ratio for each frame was calculated from the calibration curve for VOM device.[11] Also, the draw ratios values was selected between 2 and 6 with step 0.5. Figure 2 gives some examples of the contour lines for enhancement microinterferograms of iPP fibers at different drawing velocity when light vibrating parallel to the fiber axis at draw ratio 5.5.

Another sample of iPP fiber was immersed in a liquid with refractive index $n_L = 1.492$ close to the perpendicular refractive index of the fiber, at temperature $T = 30°C$. The stepper motor velocity was adjusted using the software program installed in the computer system as before. The drawing velocity was adjusted for each sample to be vary from 0.5 cm/s to 3.5 cm/s with step 0.5 cm/s. The CCD camera was adjusted to capture the video output images from the microscope field without stopping and the measurements of the refractive index of iPP

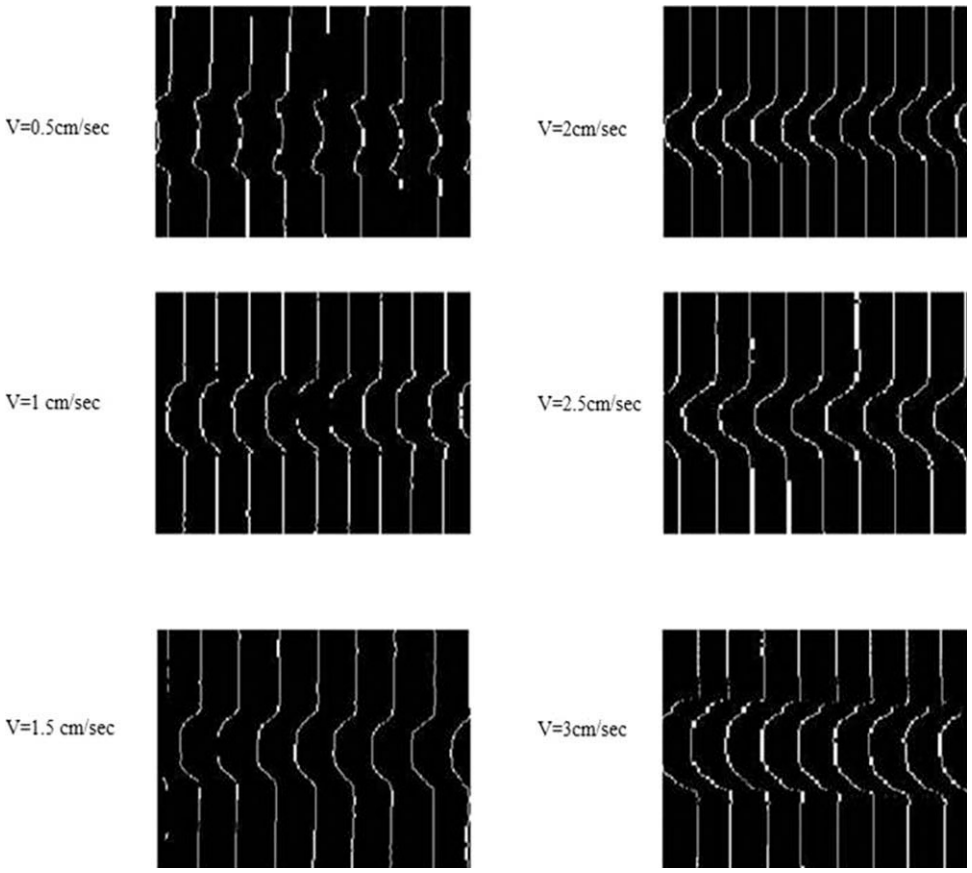

Figure 3. Examples of the contour lines obtained dynamically of the some microinterferograms of iPP fibers at different drawing velocity when light vibrating perpendicular to the fiber axis at draw ratio equals 5.5.

fiber when light vibrating perpendicular to the fiber axis were obtained. Figure 3 gives some examples of the obtained contour lines of enhancement experimental microinterferograms of iPP fibers at different drawing velocity when light vibrating perpendicular to the fiber axis at draw ratio equals 5.5.

The error in measuring the velocity (accuracy of designed VOM device or drawing resolution of the machine) is ±0.0149 cm/s.[11] The accuracy in measuring the fringe shift that is produced by multiple-beam techniques are remarkably high because the interference fringes produced from these techniques are extremely sharp and the fringe displacement is proportional to twice the phase difference introduced by the fiber. The error in the refractive index measurements is ±0.0007.[20]

RESULTS AND DISCUSSION

Table I gives the refractive index values of iPP fiber when light vibrating parallel to the fiber axis at different draw ratios and drawing velocities and Table II gives the refractive index values

Table I. The Results of the Refractive Index n^{II} of iPP Fiber When Light Vibrating Parallel to the Fiber Axis at Different Draw Ratios and Drawing Velocities

Drawing velocity cm/s DR	$V = 0.5$ cm/s n^{II}	$V = 1$ cm/s n^{II}	$V = 1.5$ cm/s n^{II}	$V = 2$ cm/s n^{II}	$V = 2.5$ cm/s n^{II}	$V = 3$ cm/s n^{II}	$V = 3.5$ cm/s n^{II}
2	1.5180	1.5184	1.5193	1.5202	1.5211	1.5220	1.5229
2.5	1.5205	1.5213	1.5222	1.5231	1.5240	1.5249	1.5258
3	1.5214	1.5222	1.5231	1.5240	1.5249	1.5258	1.5267
3.5	1.5221	1.5229	1.5238	1.5247	1.5256	1.5265	1.5274
4	1.5229	1.5237	1.5246	1.5255	1.5264	1.5273	1.5282
4.5	1.5237	1.5245	1.5254	1.5263	1.5272	1.5281	1.5290
5	1.5245	1.5253	1.5262	1.5271	1.5280	1.5289	1.5298
5.5	1.5252	1.5260	1.5269	1.5278	1.5287	1.5296	1.5305
6	1.5259	1.5267	1.5276	1.5285	1.5294	1.5303	1.5312

Table II. The Results of The Refractive Index $n^{\parallel}$ of iPP Fiber When Light Vibrating Perpendicular to the Fiber Axis at Different Draw Ratios and Drawing Velocities

Drawing velocity cm/s DR	$V = 0.5$ cm/s $n^{\perp}$	$V = 1$ cm/s $n^{\perp}$	$V = 1.5$ cm/s $n^{\perp}$	$V = 2$ cm/s $n^{\perp}$	$V = 2.5$ cm/s $n^{\perp}$	$V = 3$ cm/s $n^{\perp}$	$V = 3.5$ cm/s $n^{\perp}$
2	1.5067	1.5070	1.5063	1.5055	1.5048	1.5040	1.5033
2.5	1.5059	1.5055	1.5048	1.5040	1.5033	1.5025	1.5018
3	1.5044	1.5045	1.5038	1.5030	1.5023	1.5015	1.5008
3.5	1.5033	1.5036	1.5029	1.5021	1.5014	1.5006	1.4999
4	1.5026	1.5028	1.5021	1.5013	1.5006	1.4998	1.4991
4.5	1.5021	1.5020	1.5013	1.5005	1.4998	1.4990	1.4983
5	1.5018	1.5011	1.5004	1.4996	1.4989	1.4981	1.4974
5.5	1.5015	1.4993	1.4986	1.4978	1.4971	1.4963	1.4956
6	1.5014	1.4985	1.4978	1.4970	1.4963	1.4955	1.4948

of iPP fiber when light vibrating perpendicular to the fiber axis. It is clear from the results that, the values of the refractive index $n^{\parallel}$ is increased with increasing the draw ratio while the refractive index $n^{\perp}$ decreased. Also, the same behavior when increasing the drawing velocity. The birefringence of iPP fiber was calculated using eq. (2). Figure 4(a) shows the relation between the birefringence of iPP and the draw ratios at different drawing velocity while Figure 4(b) gives the relation between the birefringence and drawing velocity at different draw ratios. It is clear from the figure that both the draw ratios and drawing velocity affects the birefringence of iPP fiber. The birefringence increased with increasing draw ratio and drawing velocity. The birefringence of semi crystalline polymer such as iPP fiber is considered as a measure of the amorphous and crystalline regions. The increase of the birefringence indicates that the molecules constituting the fiber were oriented or aligned in parallel direction more than the perpendicular one during the online drawing process. As orientation develops by cold drawing, the units rotate towards the draw direction and become completely aligned at the maximum achievable orientation.[21,22] As the velocity of drawing increases the orientation process or the alignment of molecules toward the drawing direction increases

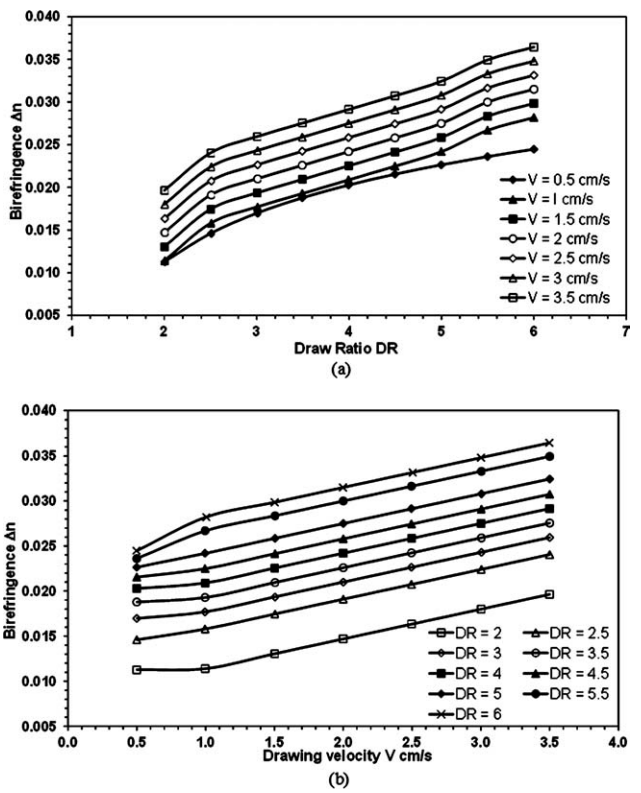

Figure 4. (a) The relation between the birefringence of iPP fiber and the draw ratios DR at different drawing velocity and (b) The relation between the birefringence and drawing velocity at different draw ratios.

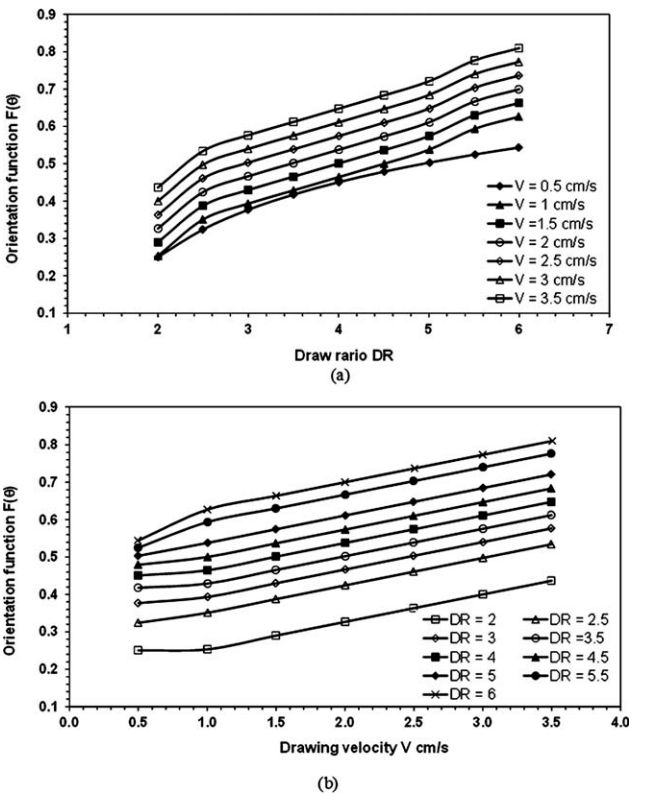

Figure 5. (a) The graphical presentation of the optical orientation function $F(\theta)$ of iPP fiber and the draw ratio DR and (b) shows the graphical relation of the same quantity and the drawing velocity.

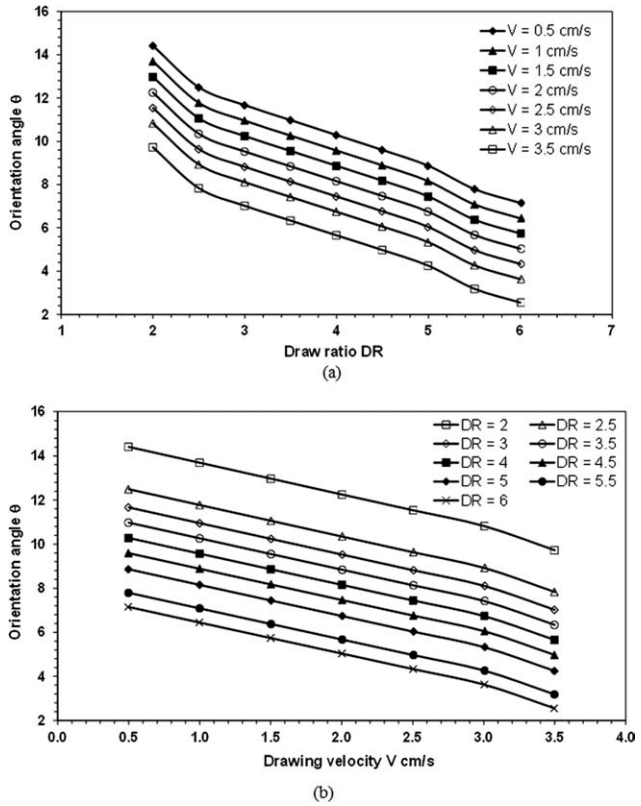

Figure 6. (a) The graphical presentation of the orientation angle (θ) of iPP fiber and the draw ratio and (b) shows the relation between the orientation angle (θ) and the drawing velocity.

and becomes the more occurring phenomena. So that the birefringence increases rapidly with increasing both the draw ratio and drawing velocity.

To study the influence of the mechanical drawing and drawing velocity on the molecular structure of iPP fibers, the results of the birefringence were utilized to calculate the optical orientation function using eq. (3). Figure 5(a) shows the graphical presentation between the optical orientation function $F(\theta)$ and the draw ratio DR while Figure 5(b) shows graphical relation of the same quantity and the drawing velocity. It is clear that, as the values of both the draw ratio and the velocity of drawing increase, the orientation of the chains increases. The results of the calculated optical orientation function $F(\theta)$ were utilized to calculate optical orientation angle (θ) using eq. (4). Figure 6(a) gives the graphical presentation between the orientation angle (θ) and the draw ratio while Figure 6(b) gives the relation between the orientation angle (θ) and the drawing velocity. From Figures 5 and 6, it clear that, the optical orientation function $F(\theta)$ increased with increasing both the draw ratio DR and drawing velocity while the orientation angle decreased with increasing both the draw ratio DR and drawing velocity. This indicates that, the molecules constitute the iPP fibers affected by mechanical cold drawing and drawing velocity. They oriented in the direction of drawing. So that the orientation function increased and the orientation angle decreased due to drawing process. Also, it obvious that, the influence of the draw ratio values is more than the influence of the drawing velocity on the orientation of molecules of iPP fiber.

Whereas the degree of orientation always increases in the course of drawing process, crystallinity can change in both direction. Using eqs. (5)–(9), the percentage of the volume fraction of crystalline regions χ_v% , amorphous regions $(1-\chi_v)$%, density ρ and the mean square density fluctuation $\langle\eta^2\rangle$ were calculated at different draw ratios and drawing velocity. Figure 7(a) gives the graphical presentation between the percentage of the volume fraction of crystalline regions χ_v% and the draw ratio DR while Figure 7(b) gives the relation between the percentage of the volume fraction of crystalline regions χ_v% and the drawing velocity. It clear that, the percentage of volume fraction of crystalline regions χ_v% decreased nonlinear with increasing the draw ratio DR but the same amount decreased linearly with increasing the drawing velocity. Figure 8(a) shows the graphical relation between the percentage of the volume fraction of amorphous regions $(1-\chi_v)$% and the draw ratio while Figure 8(b) gives the relation between the percentage of the volume fraction of amorphous regions $(1-\chi_v)$% and the drawing velocity. The percentage of volume fraction of amorphous regions $(1-\chi_v)$% increased nonlinearity with increasing the draw ratio DR but linearly increased with increasing the drawing velocity. The calculations of χ_v% and $(1-\chi_v)$% from the density data interpret the physical and structural properties of semicrystalline iPP

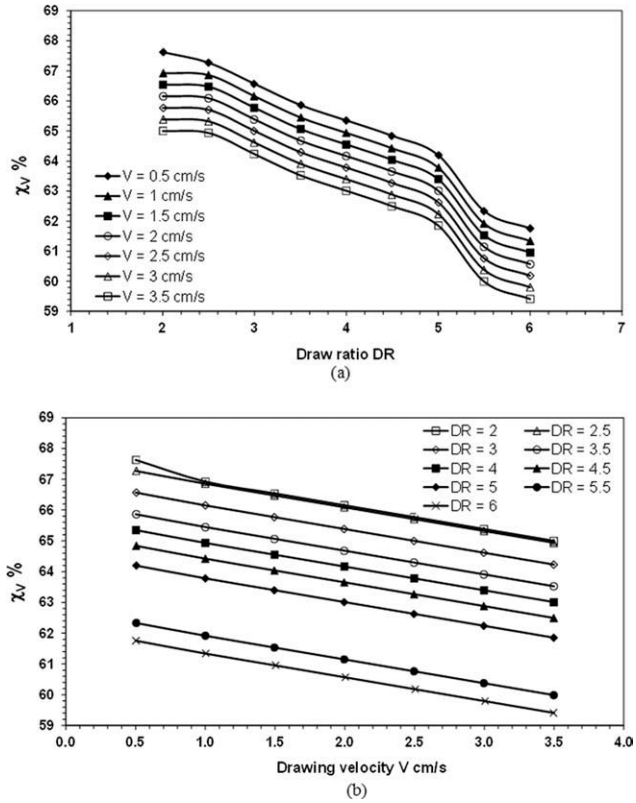

Figure 7. (a) The graphical presentation between the percentage of the volume fraction of crystalline regions χ_v% of iPP fiber and the draw ratio DR and (b) shows the relation between the same quantity and the drawing velocity.

Applied Polymer SCIENCE

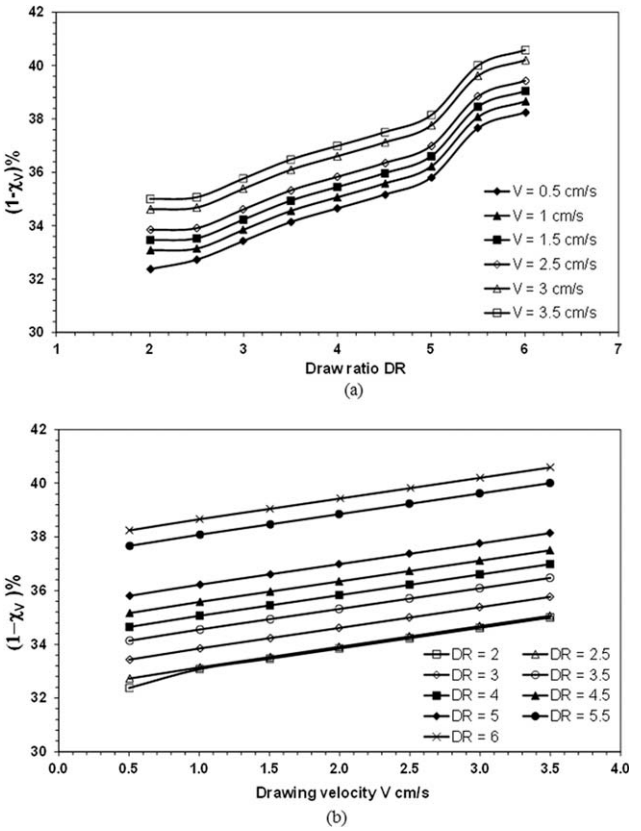

Figure 8. (a) The graphical relation between the percentage of the volume fraction of amorphous regions $(1\text{-}\chi_v)\%$ of iPP fiber and the draw ratio while (b) shows the same quantity and the drawing velocity.

fiber based on a two-phase model. In this model, it is assumed that the polymer consists of an amorphous and a crystalline phase. The properties of each phase are independent of the presents and amount of the other phase. Generally, It is obvious that the influence of increasing the draw ratio of iPP fiber on the crystallinity values is greatly observed than the influence of increasing drawing velocity. Density and the mean square density fluctuation are related primarily to crystallinity and must behave similarly. Figure 9(a) shows the graphical presentation of the density ρ of iPP fiber and the draw ratio DR while Figure 9(b) shows the variation of the same quantity with the drawing velocity. Also, Figure 10(a) shows the graphical presentation of the mean square density fluctuation $\langle \eta^2 \rangle$ and the draw ratio DR of iPP fiber while Figure 10(b) shows the variation of the same quantity with the drawing velocity. It is clear that density values decreased while the mean square density fluctuation $\langle \eta^2 \rangle$ increased nonlinearity with increasing the draw ratio DR but the same quantities decreased and increased with increasing the drawing velocity. From studying the influence of drawing conditions on the molecular structure of iPP fiber, it may conclude that, the deformation of iPP fiber consists of destruction of the original crystal structure and rebuilding of a new defective structure oriented in the direction of drawing. This needs a farther experimental measurements to confirm this prediction.

CONCLUSIONS

Isotactic polypropylene iPP fiber is of semicrystalline structure. The mechanical cold drawing process has great effects on the molecular structure of iPP fiber. The influence of increasing the draw ratio, on the physical structure variation, is more obviously than the influence of increasing the drawing velocity of iPP fiber. The VOM device attached with the automated multiple beam micro-interferometric technique is more suitable and accurate technique enable the continuous monitoring of the fiber structure variations during the drawing process. From the measurement carried out, the following conclusions can be drawn:

1. The orientation increased with increasing both the draw ratio and drawing velocity.
2. The crystallinity of iPP fiber decreased with increasing both the draw ratio and drawing velocity.
3. The overall density of iPP fiber decreased while the mean square density fluctuations increased with increasing both the draw ratio and drawing velocity. These results confirm the decrease in the overall crystallinity and other physical structure variations of iPP fiber during the drawing process.
4. This study shows that, application of the VOM device attached with the automated multiple-beam technique could be successfully used for detecting any physical deformations during the cold drawing process.

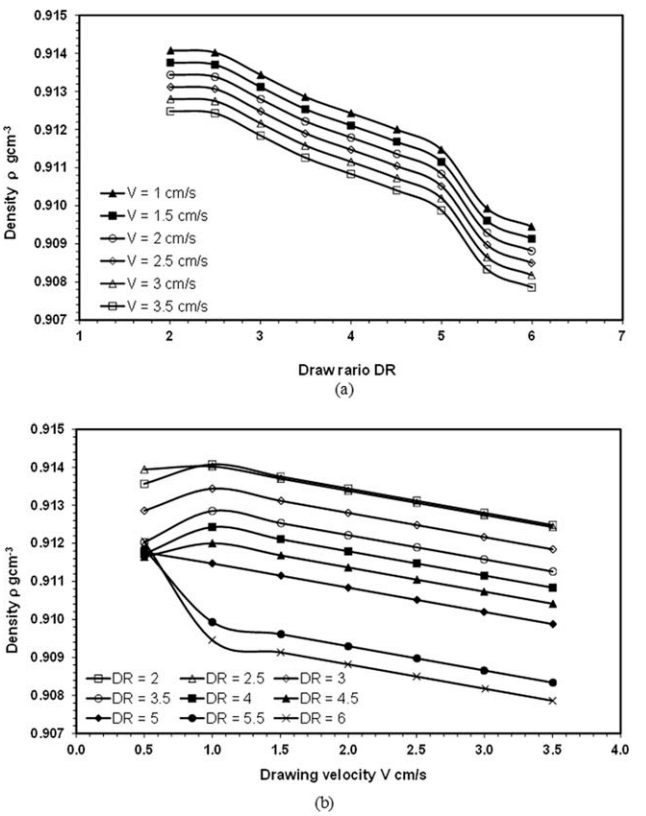

Figure 9. (a) The graphical presentation of the density ρ of iPP fiber and the draw ratio DR while (b) shows the variation of the same quantity with the drawing velocity.

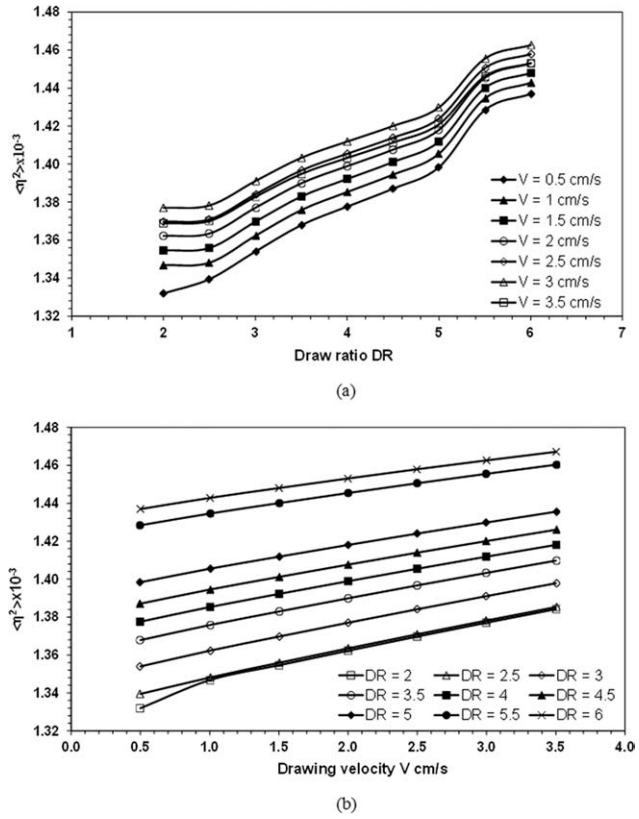

Figure 10. (a) The graphical presentation of the mean square density fluctuation $\langle \eta^2 \rangle$ and the draw ratio DR of iPP fiber while (b) shows the variation of the same quantity with the drawing velocity.

ACKNOWLEDGMENTS

The authors would like to acknowledgment a dept of gratitude and appreciation to Professor A.A. Hamza Professor of physics and the President of British University in Egypt for their guidance and useful discussions.

REFERENCES

1. Paukkeri, R.; Vaananen, T.; Lehtinen, A. *Polymer.* **1993,** *34*, 2488.
2. Bogoeva-Gaceva, G.; Grozdanov, A. *J. Serb. Chem. Soc.* **2006,** *71*, 483.
3. Available at: http://en.wikipedia.org/wiki/Tacticity#Isotactic_polymers.
4. Junkasem, J.; Menges, J.; Supaphol, P. *J. Appl. Polym. Sci.* **2006,** *101*, 3291.
5. Xixiong, Z. *J. Polym. Sci. B Polym. Phys.* **1993,** *31*, 1667.
6. Lee, S. Y.; Bassett, D. C.; Olley, R. H. *Polymer.* **2003,** *44*, 5961.
7. Walezak, Z. K. Formation of Synthetic Fibers, Gordan and Breach Scientific Publication: New York, **1977;** Chapter 6.
8. Barakat, N.; Hamza, A. A. Interferometry of Fibrous Materials, Bristol: Adam Hilger, New York, **1990.**
9. El-Bakary, M. A. *Opt. Lasers Eng.* **2008,** *46*, 328.
10. El-Bakary, M. A. *Optics Laser Technol.* **2007,** *39*, 1273.
11. Sokkar, T. Z. N.; El-Tonsy, M.; El-Bakary, M. A.; El-Morsy, M. A.; Ali, A. M. *Optics Laser Technol.* **2009,** *41*, 317.
12. El-Dessouky, H. M.; Mahmoudi, M. R.; Lawrence, C. A.; Lewis, E. L. V.; Voice, A. M.; Ward, I. M. *Polym. Eng. Sci.* **2010,** 200.
13. Hemsley, D. A. Applied Polymer Light Microscopy, Elsevier Science Publishers: London, **1989;** p 94.
14. De Vrise, H. *Colloid. Polymer Sci.* **1979,** *257*, 226.
15. Cheremisinoff, N. P. Handbook of Polymer Science and Technology, CRC Press: New York, **1989;** Vol. *2.*
16. Kudrna, M.; Mitterpachova, M. *Colloid. Polym. Sci.* **1983,** *261*, 903.
17. Schael, G. W. *J. Appl. Polym. Sci.* **1968,** *12*, 903.
18. Ficher, E. W.; Fakirov, S. *J. Mater. Sci.* **1975,** *11*, 955.
19. Hamza, A. A.; Sokkar, T. Z. N.; Mabrouk, M. A.; El-Morsy, M. A. *J. Appl. Polym. Sci.* **2000,** *77*, 3099.
20. Hamza, A. A.; Kabeel, M. A. *J. Phys. D Appl. Phys.* **1986,** *19*, 175.
21. Hamza, A. A.; Sokkar, T. Z. N.; El-Morsy, M. A.; Raslan, M. I.; Ali, A. M. *Opt. Commun.* **2010,** *283*, 1684.
22. Hamza, A. A.; Sokkar, T. Z. N.; El-Bakary, M. A.; Ali, A. M. *Opt. Laser. Technol.* **2010,** *42*, 703.